A REVIEW OF AERONAUTICAL FATIGUE INVESTIGATIONS IN ISRAEL

APRIL 2001 – MARCH 2003

Compiled by:
Abraham Brot
Engineering Division
Israel Aircraft Industries
Ben-Gurion Airport, Israel

abrot@iai.co.il

SUMMARY

This review summarizes fatigue and fracture-mechanics investigations that were performed in Israel during the period April 2001 to March 2003. The review includes contributions from Israel Aircraft Industries Ltd. (IAI), Israel Air Force (IAF), Technion – Israel Institute of Technology, Tel-Aviv University and Ben-Gurion University.

Presented at the 28th ICAF Conference
Lucerne, Switzerland
6 May 2003

TABLE OF CONTENTS

A REVIEW OF AERONAUTICAL FATIGUE INVESTIGATIONS IN ISRAEL APRIL 2001 – MARCH 2003

11.1 INTRODUCTION

The Israel National Review summarizes work performed in the field of aeronautical fatigue in Israel during the period April 2001 to March 2003. The previous National Review [1] covered aeronautical fatigue activities up to March 2001. The following organizations contributed to this review:

Israel Aircraft Industries Ltd. (IAI)
Israel Air Force (IAF)
Technion – Israel Institute of Technology
Tel-Aviv University
Ben-Gurion University

The National Review was compiled by Abraham Brot of IAI (abrot@iai.co.il).

11.2 FATIGUE ANALYSIS AND LIFE EXTENSION

11.2.1 Optimum Laser Treatment of Metals (E. Altus and E. Konstantino, Technion)

This investigation is a continuation of work reported upon in the Israel National Review that was presented to the 27th ICAF Conference [1]. A Laser Surface Treatment (LST), which enhances fatigue resistance of Titanium 6Al-4V alloy, has been studied by 1.8 kW CW CO_2 Laser. The aim of the study is to find optimal conditions of treatment, which will extend the material resistance to fatigue failure, and explore the mechanisms involved. The LST was applied to "Three Point Bend" specimens loaded cyclically (R=0.1, $0.7\sigma_y$ near surface stresses), at different stages of fatigue life. Temperature surface fields were found by infrared camera. Two basic mechanisms were identified: one is related to Healing Mechanism (HM), which "erases" prior fatigue damage up to a certain level, and the other is connected to Microstructure Mechanism (MM). Healing was found to be effective for surface temperatures above 400°C. In most cases, microstructure changes had a negative effect on fatigue resistance except for temperatures lower than 600°C and specific laser conditions. The combination of both mechanisms lead to optimal LST of 2sec and 0.85kW/cm^2, for which a 50% increase in fatigue life was found to be due to MM, in addition to a full healing. A positive correlation between hardness and fatigue life was also found. The results of this investigation were published in [2].

11.2.2 Nonlinear Differential Equation for Fatigue Damage Evolution by a Micromechanic Model (E. Altus, Technion)

A 1-D discrete (cycle-by-cycle) micromechanical fatigue model, which represents a material made from an ensemble of elements having statistical (Weibull) strength distribution, has been developed in previous works. In the present study, the recursive type equations have been transformed into a continuous form, leading to a nonlinear second order differential equation of damage evolution (stiffness reduction), for which an exact solution is possible in some cases. By an analytical treatment, explicit relations between microscale parameters and a well-known macro S-N material response were found. Two major results have been obtained analytically: a) A relation between the ensemble statistical strength distribution and a commonly observed fatigue power law, and b) A relation between the scale of microfailure probability of neighbor elements and the macro endurance limit phenomenon, *without* any a priori condition. In addition, the model predicts three distinct types of fatigue damage evolution characteristics, commonly seen in fatigue tests. At high stresses, damage rate increases monotonically until failure. At medium level stresses, three regions (primary, secondary and tertiary) are observed, resembling strain-time creep response. Finally, at stresses lower than the endurance limit, an exponentially decaying behavior is observed. The results of this study were published in [3].

11.2.3 Two-Level Fatigue Loading of Mg Alloys: Micromechanic Modeling vs. Experiments (E. Altus, Z. Gerstman, A. Golubchick, Technion)

A statistical micromechanic fatigue model developed in the past, showed some of the main features of macro fatigue behavior like S-N power law, endurance limit, Goodman diagram, etc. The model correlates micro statistical damage parameters, such as local probabilities of failure and neighbor element interaction with macro response characteristics, seen in fatigue experiments. The cycle-by-cycle recursive evolution equation of the model has been recently transformed to a nonlinear differential equation, which enabled a simple analytic solution. Using this solution, a two level (H-L) fatigue failure case is treated analytically. A simple design formula is received, which is based solely on the S-N data, without any additional material parameters. Specifically, the model predicts a generalized "Miner type" behavior, which is controlled on the micro-level by the very basic strength dispersion factor of the microelements, and on the macro-level by the S-N slope. The proposed H-L predictions were tested by fatigue experiments on two Magnesium alloys (AZ31 and AM50). Results [4] showed good correlation, in spite of the natural large scatter.

11.2.4 Cracking of Autofrettaged Thick-Walled Cylinders (M. Perl et al, Ben-Gurion University)

A series of investigations were performed, all dealing with thick-walled cylindrical pressure vessels [5] – [8]. These investigations are a direct continuation of work that was presented in the previous Israel National Review [1]. Although this work does not deal strictly with aeronautical fatigue, it was included in this review because the autofrettage technique is very similar to the cold-expansion method used extensively in the aircraft industry.

Three-dimensional finite-element models were built to study stress intensity distributions for arrays of cracks along the bore of an autofrettaged cylinder [5]. The ANSYS 5.3 Finite-Element Code was used for the study. The number of cracks ranged from one to 180. More than 200 different combinations of crack depth, crack shape and levels of autofrettage were studied parametrically. The results clearly showed the importance of autofrettage in reducing the effective stress intensity factor. A follow-up investigation was performed, in which the combined effect of autofrettage and internal pressure was studied [6]. The results of this study enable the prediction of crack growth rate and fatigue life for a pressurized autofrettaged cylinder.

This investigation was further extended [7] by simulating the effect of multiple axial erosions of various configurations on the fatigue life of a pressurized autofrettaged cylinder. The problem is simulated by a two-dimensional finite-element model. The results show, that for certain erosion configurations, the fatigue life of the cylinder may decrease by up to an order-of-magnitude. A further improvement was made in [8] by simulating the axial erosions by a three-dimensional finite-element model. The results indicated that, for specific erosion configurations, the two-dimensional solution was unconservative compared to the three-dimensional solution.

11.2.5 An Evaluation of Several Retardation Models for Crack Growth Prediction under Spectrum Loading (A. Brot and C. Matias, IAI)

It is well established that, under spectrum loading, load-interactions occur which generally retard the rate of crack growth. This means that the crack growth rate is usually considerably slower than predicted by da/dN vs. ΔK data for the individual loads. This effect can be very significant — for certain types of loading spectra, the life increase due to retardation may be a factor ranging from 2 to 5.

Unfortunately, it is very difficult to predict a priori the extent of retardation that can be expected for a specific combination of alloy, loading spectrum, stress level and crack configuration. Several retardation models have been proposed in the past 30 years, which are semi-empirical models since their dominating parameters must be “calibrated” for a specific alloy, loading spectrum, stress level and crack configuration combination. These models have limited value in predicting crack growth behavior

The present study included four widely used aluminum alloys, which have been tested under five distinct spectrum types. The test coupons include two crack configurations: Center cracked tension (CCT) coupon and open hole cracked tension coupon. The test results were evaluated using several state-of-the-art load-interaction models including the “Strip-Yield Model” (NASA and ESA versions, SY-N and SY-E), the “Generalized Willenborg Model” (GW) and the “Modified Generalized Willenborg Model” (MGW). In all cases, the emphasis was on using the above retardation models with a minimal need for calibration.

Predictions of the four retardation models gave large variations compared to crack growth measurements, over the entire range of tests. Figure 1 shows typical test results compared to unretarded calculations and retardation predictions using the four models that were studied. The challenge was to examine all the results and to attempt to find the patterns of the behavior.

All the predicted crack growth lives were compared to the measured results, for each of the four retardation models that were studied. Statistical analyses of the results were performed and showed that all the retardation models, on the average, correlated reasonably well with the range of test data. However, the "Strip-Yield Model" (NASA) gave the least variation, as is shown in Figure 2.

Examining the results from a spectrum point of view reveals some interesting trends: The study indicates that the extent of retardation generally decreases as the spectrum that is being implemented has a higher mean stress-ratio.

The retardation models, in general, can reasonably predict crack growth for spectra having stress-ratios in the range of -1 to 0, and have a lower degree of accuracy to predict the extent of retardation for spectra having positive stress-ratios.

The results were examine statistically and revealed that for one of the loading spectrums, on average, the retardation models predicted very accurately the degree of retardation but displayed an extraordinary large degree of variation. For another loading spectrum type, little results variation was noted, but the average prediction was very conservative. The reasons for these results are not evident.

Examining the results from a material point of view, shows that for two of the materials tested the predictions on average were accurate with a quite large variation, and for the other two materials tested the predictions on average were somewhat conservative, with much smaller variation.

Significant differences were found in predictions for CCT coupons compared to predictions for open hole coupons. The CCT coupons seem to give more reliable results.

The results of this study were presented at the 2002 USAF Aircraft Structural Integrity Program Conference [9] and at the 43rd Israel Annual Conference on Aerospace Sciences [10].

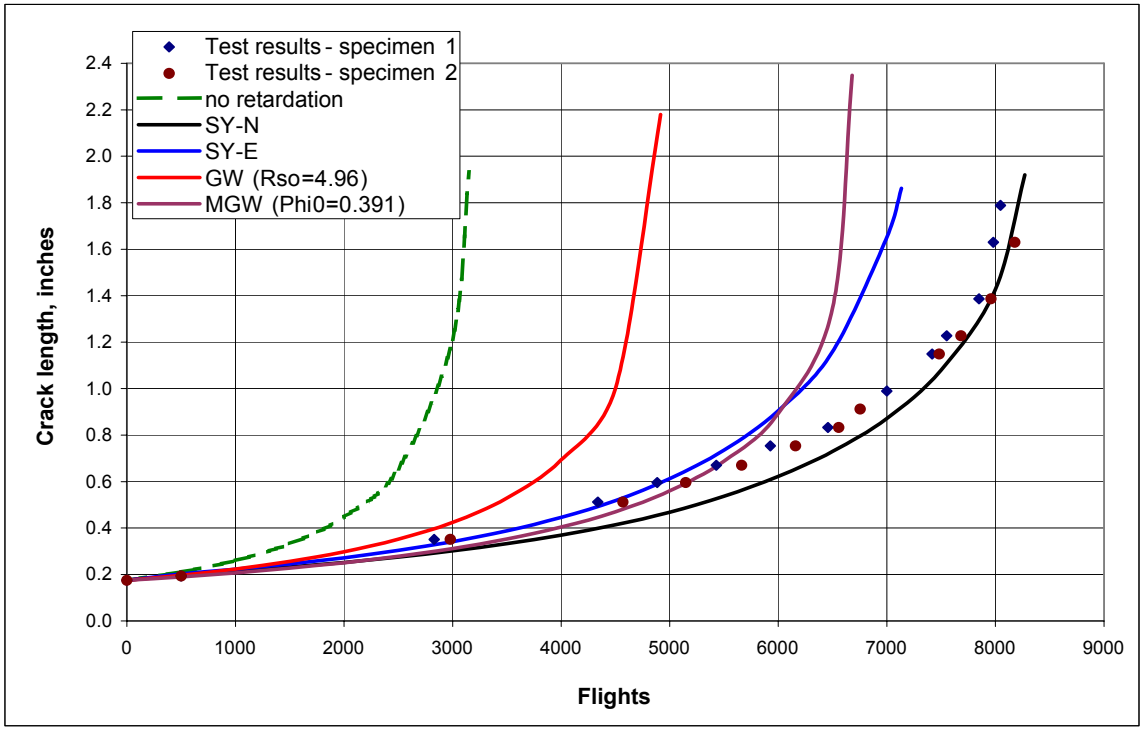

Figure 1: Crack Growth of 2024-T351 CCT Coupons Under the "Fighter Aircraft Maneuver Spectrum"

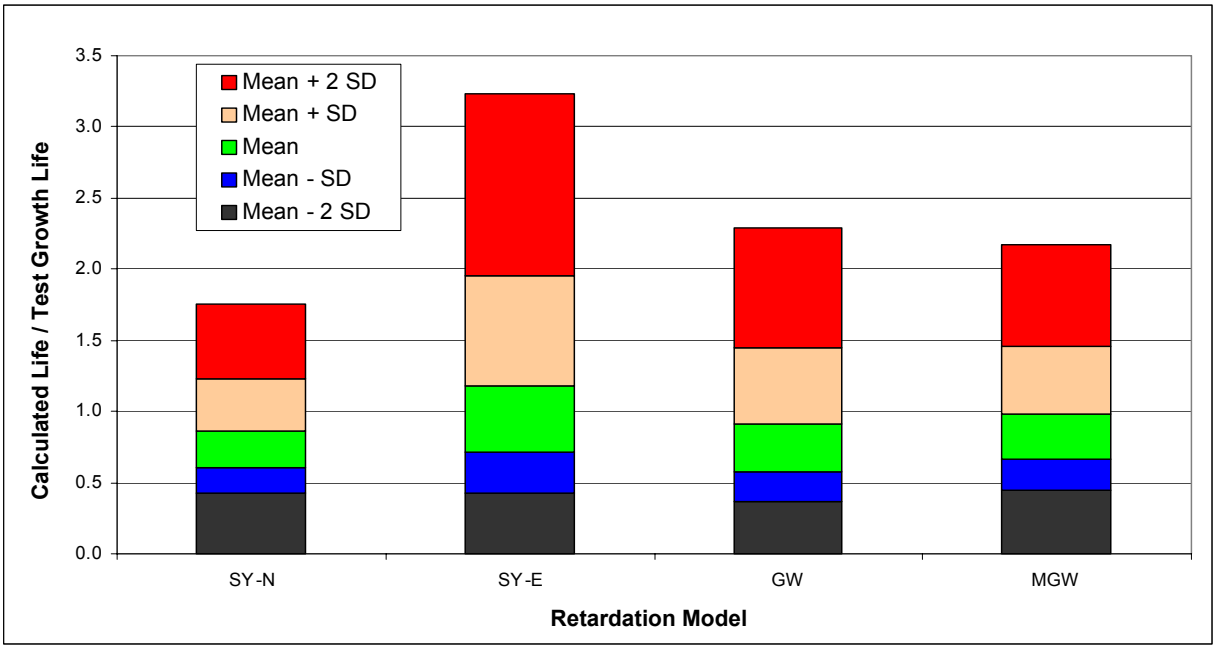

Figure 2: Retardation Model Performance Comparison

11.2.6 Determining Crack-Arrest Capability of Integrally Machined Structures by Analysis and Testing (C. Matias and A. Brot, IAI)

IAI has begun a study into the crack-arrest capability of integrally machined structures. Among the configurations to be studied is a bulkhead having integral ribs subjected to pressure loading. A finite-element model was built using StressCheck p-version software. A crack is introduced into one of the stiffening ribs and the crack is progressively lengthened. Stress-intensities and stress levels on the adjacent ribs are calculated by the software as the cracking is progressively lengthened. Figure 3 shows a typical result of the p-version FEM. It should be noted that sophisticated nature of the elements (up to 8^{th} order polynomial) allows the use of relatively few elements without compromising accuracy of the solution.

The aim of the study is to determine parametrically the optimum geometric configuration of the structure (rib height, width and spacing) to provide reliable crack-arrest behavior. A series of tests are planned in order to verify the analytical results.

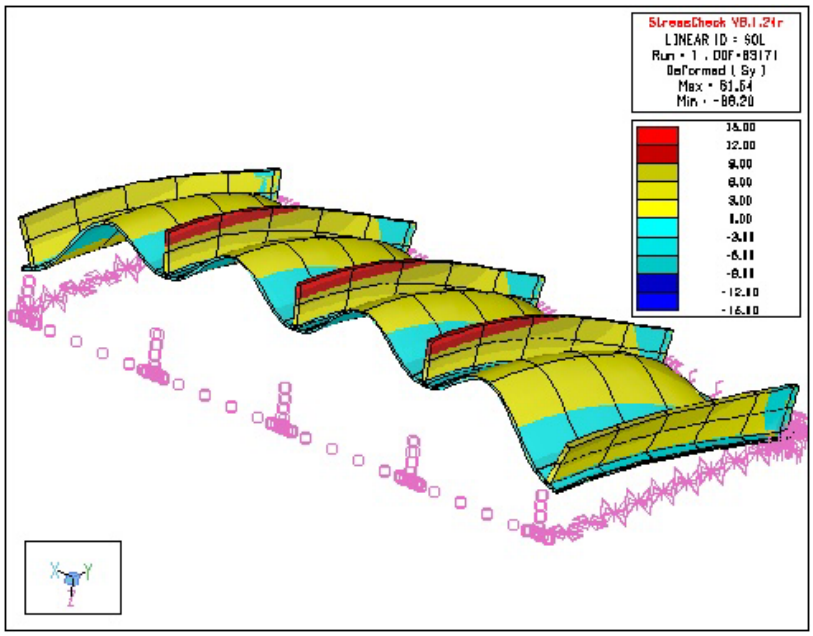

Figure 3: Finite-Element Model (p-version) of a Cracked Integral Structure

11.3 AIRCRAFT PROJECTS

11.3.1 G200 Executive Jet Fatigue Substantiation Program (S. Afnaim and A. Brot, IAI)

The G200 (formerly known as the Galaxy) is a wide-body executive jet, developed by Israel Aircraft Industries and subsequently incorporated into the Gulfstream Aerospace Corporation family. The G200 has a transatlantic range and a maximum cruise speed of Mach 0.85. It can transport up to 18 passengers in a corporate configuration and up to nine passengers in an executive configuration. The G200 is powered by two PW306A jet engines. The G200 primary structure is metallic except for the ailerons, elevators and rudder that are manufactured from composite materials.

The G200 airframe structure has been substantiated to the FAR-25 damage-tolerance requirements. In addition, fatigue and damage-tolerance component and full-scale tests were performed in order to support the damage-tolerance analyses. Several of these tests were described in previous National Reviews [1]. This review describes activities performed since 2001.

11.3.1.1 Full-Scale Fatigue Test

The G200 has been designed to a service life objective of 36,000 hours and 20,000 flight cycles. In order to substantiate this life objective, the aircraft was tested in a full-scale fatigue test for a duration of two lifetimes.

The test-article for the full-scale fatigue test consists of all the structural members of the fuselage and both wings. The empennage is being fatigue tested separately. The test aircraft was mounted to the test fixture at the nose landing gear attachment and at the engine mount fittings. Figure 4 is a photo of the G200 aircraft mounted in its loading fixture.

Figure 4: G200 Full-Scale Fatigue Test Aircraft

The fatigue spectrum loading consists of randomly selected flight-by-flight sequences, reflecting the anticipated usage of the aircraft. A flight consists of the various flight and ground events that the aircraft experiences. Approximately 20 events per flight have been included in the 2000 flight spectrum block.

The test-article was divided into 29 loading zones, each of which is independently loaded during each event of the spectrum, using 42 servo-hydraulic actuators. In addition, the passenger cabin and baggage compartment is pressurized, using compressed-air during the airborne events of the spectrum. The zone loading for each event was determined using a "constrained least-square error method" which minimized deviations in loading of the important structural parameters. Approximately 1500 strain-gages have been bonded to the test-article, mainly to monitor the onset of cracking.

Testing began in December 1998 and has successfully completed the 40,000 flights by December 2002. Strains were monitored every 500 flights; whenever a large deviation in strains was observed, the area was inspected for cracks. NDI was performed at 2500 flight intervals.

A number of cracks have been detected during the full-scale test, in the following areas:

- Baggage compartment
- Nose landing gear bay in the forward fuselage
- Cabin forward and aft pressure bulkheads
- Windshield sill beam
- Emergency exit door stops

In all cases, the crack growth rates were sufficiently slow, as not to result in any danger. Nevertheless, design changes were introduced to improve the durability of the structure in all these areas. These design changes were introduced in new production and will be retrofitted to the existing fleet. Strain levels were measured in the region of the design changes and, in all cases, were found to be sufficiently low to insure an adequate fatigue life.

A *selected* teardown inspection will be performed in order to determine if additional areas were cracked during the two-lifetime test, in order to establish the absence of *widespread fatigue damage*.

11.3.1.2 Empennage Fatigue and Damage-Tolerance Test:

The entire empennage assembly has been mounted to an aft fuselage structure for fatigue testing, as is shown in Figure 5. The test includes the elevator and rudder, which have been manufactured from composite materials. The loading spectrum includes vertical and lateral loading resulting from gust and maneuvers as well as measured buffeting loads arising from thrust reverser deployment. The horizontal and vertical tails were divided into ten loading zones, each of which is independently loaded during each event of the spectrum, using servo-hydraulic actuators. Approximately 200 strain-gages were bonded to the structure for strain monitoring, which is performed every 1000 flights. The test-article is inspected for cracks at 5000 flight intervals.

The composite material elevator and rudder is being tested for damage-tolerance under manufacturing and service-inflicted damage as well as under barely-visible impact damage.

Figure 5: G200 Empennage – Fatigue and Damage-Tolerance Test

The G200 Empennage fatigue test started in December 1998. The aim of the test is to follow a two-lifetime (40,000 flight) fatigue test by one lifetime of damage-tolerance testing (total of 60,000 flights). Following the completion of two lifetimes, 30 flaws were introduced at specific locations on the empennage metallic and composite structures; testing has reached 43,000 flights. These flaws are monitored for crack growth on the metallic structure and delaminations on the composite structures.

11.3.1.3 Main Landing-Gear Fatigue Test

The main landing gear spectrum loads are applied in the vertical, drag and side directions on the Galaxy landing gear. A truncated fatigue-load spectrum of the ground-loads is used for this test, after combining and simplifying some of the ground-operations. Each flight-cycle consists of taxi, turning, braking, pivoting, rotation and landing-impact events. The test spectrum was truncated to include approximately 20 events per flight. Groups of 1,000 of these flights were assembled into each block of flight-cycles for the fatigue-test load-spectrum.

The G200 landing gear was originally scheduled to be fatigue tested to five lifetimes (100,000 flights). Because of a weight increase of the G200, and in order to demonstrate growth potential, a total of 150,000 flights (7.5 lifetimes) will be performed. By January 2003, the main-gear test has reached 130,000 flights with no significant failures or detectable damage.

11.3.1.4 Wing Rib 2 Fatigue Test

An independent test program was performed in order to study the fatigue characteristics of a potentially critical location on the lower wing skin, in the area of Rib 2. Two lower skin test components, simulating the Rib 2 area, have been manufactured. The first component was tested with initial flaws introduced at the most critical locations. Spectrum loading was applied during the test and a residual strength load was applied at the end of the component test. The results showed that the lower skin crack arrests as it approaches the wing rib. The crack continued to remain in an arrested state, when the residual strength conditions were applied. The test demonstrated that the wing's inherent damage-tolerance was not compromised by the presence of cracks on the lower wing skin.

A second component will be tested in order to confirm the adequacy of a planned repair of this location.

11.3.2 G150 Executive Jet Fatigue Substantiation Program (S. Afnaim and A. Brot, IAI)

Israel Aircraft Industries and Gulfstream Aerospace Corporation are currently jointly developing the G150, midsize executive jet. The G150 will have transcontinental range and a maximum cruise speed of Mach 0.85. It can transport up to eight passengers in an executive configuration. The G150 will be powered by two TFE 731 jet engines. The G150 primary structure will be metallic except for the ailerons and elevators that are manufactured from composite materials.

Figure 6 illustrates the configuration of the G150 executive jet.

The G150 will be certified to the FAR-25 Regulations, with a first flight scheduled for the fourth quarter of 2004 and FAA certification during 2005.

As part of the damage-tolerance certification, a G150 test-article will be fatigue tested to two lifetimes (40,000 flights).

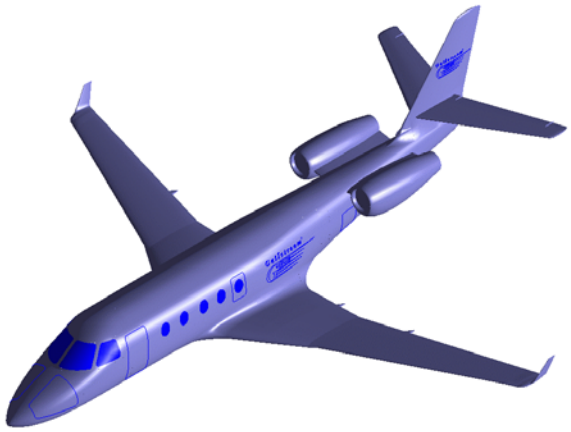

Figure 6: G150 Midsize Executive Jet

11.3.3 A Damage-Tolerance Approach for Life Extension of a Helicopter Pitch-Housing (I. Kochavi, M. Mileguir, IAF)

The pitch-housing component in the IAF AH-64A Apache helicopter (Figure 7) is currently replaced by the IAF at specific intervals, based on the "safe life" replacement policy recommended by the manufacturer. This policy was thought to be unnecessarily conservative and costly. An investigation to extend the service life of the 7049-T73 aluminum pitch-housing by using an "on-condition" replacement procedure was performed. Up to now, no pitch housing removed from IAF aircraft has exhibited fatigue cracks.

Spectrum evaluation and crack growth analysis of the pitch-housing lug was performed in order to determine whether the component has the potential to be used safely for additional flight hours by inspecting periodically for cracks, as was described in the 2001 Israel National Review [1].

A three-stage test program is presently underway in order to verify the analytical results, as was described in the 2001 Israel National Review [1].

A final decision on implementing this life extension program on the IAF fleet awaits the results of these on-going flight spectrum tests.

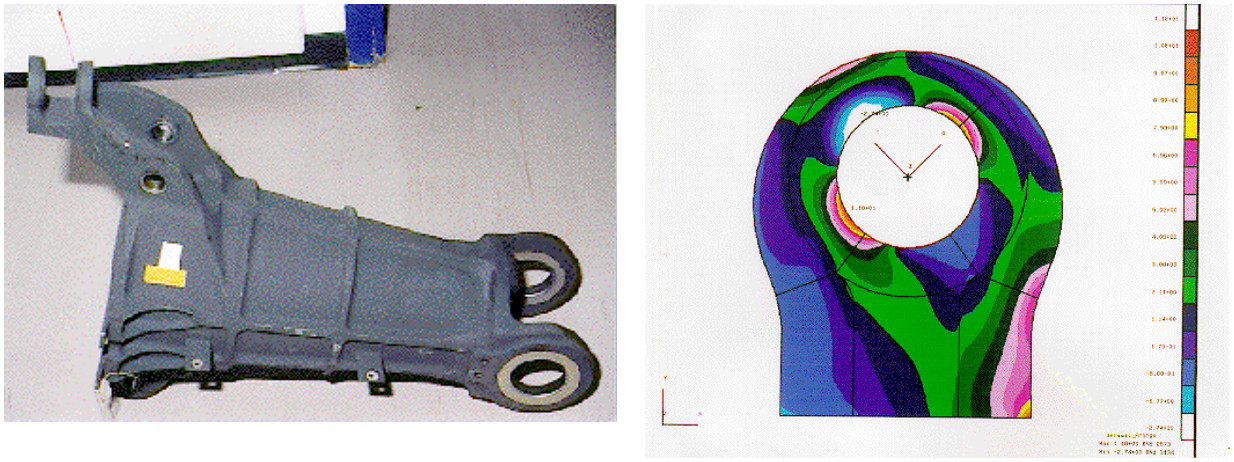

Figure 7: IAF AH-64A Apache Helicopter Pitch-Housing Component and Stress Distribution in Lug

11.3.4 Design Substantiation and Application of a Boron-Epoxy Patch Repair on an F-16 Upper Fuselage Skin (I. Kressel, IAI / I. Cohen, IAF / S. Gali, Consultant)

The F-16 upper fuselage skin suffers from fatigue cracks, initiated from fastener holes and access panels corners, as is shown in Figure 8. The Israeli Air Force (IAF) has also experienced numerous fatigue cracks at the skin splice at fuselage station 341.8. Available repair kits are expensive, labor intensive and with long lead-time. A bonded repair concept was selected as a temporary repair in order to avoid drilling in the original structure and allowing the possibility of removing the repair to accommodate a standard permanent repair.

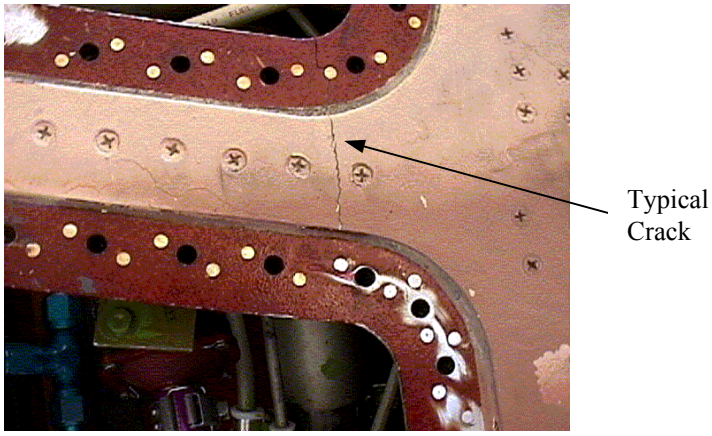

Figure 8: F-16 Fuselage Upper Skin at Station 341.8

The main design criteria were as follows:

Implementation of the repair on a cracked skin (after the crack has been removed by milling)

- Repair must be reliable until a permanent repair can be implemented.
- A 20% to 30% reduction of stresses at the critical areas is needed.
- Use of known, suitable for field application, surface treatment and curing cycle for bonding repair.
- Use of standard NDT methods for patch and skin inspections.

A joint team composed of Israel Aircraft Industries (IAI) and IAF specialists performed the design, substantiation and application of the repair. Currently the repair has been implemented on one aircraft and is being monitored periodically in order to detect disbonds and delaminations.

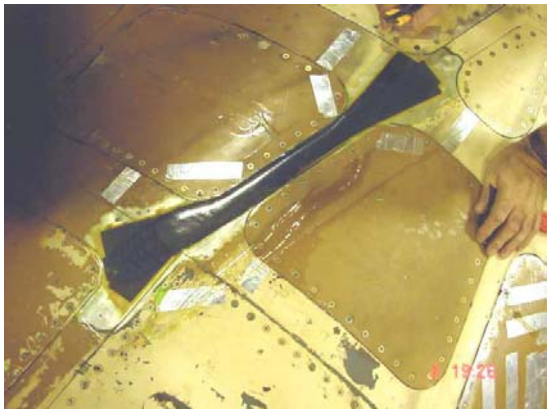

The major challenge in designing a repair for this location is the limited area available for bonding. The ligament between the access panels is only 40mm wide. In order to get the required stiffness, a 4mm Boron-Epoxy co-cured patch was designed. The Boron-Epoxy tape was selected as the repair system because of its high strength and stiffness. The use of Boron, as compared to Carbon, also reduces the residual thermal stresses induced during the cure cycle due to the difference in the thermal expansion coefficient between the basic aluminum aircraft structure and the composite repair. Special effort in the design phase was dedicated to the drop-off area of the patch because of the limited area available. Figure 9 shows the repair on the F-16 aircraft.

Figure 9: F-16 Boron-Epoxy Patch Repair

A Finite-element model, representing all structural members at the repair area was developed. Comparison between stresses distribution before and after repair application was performed. The effect of the repair on the surrounding structure was also investigated through the finite-element analysis.

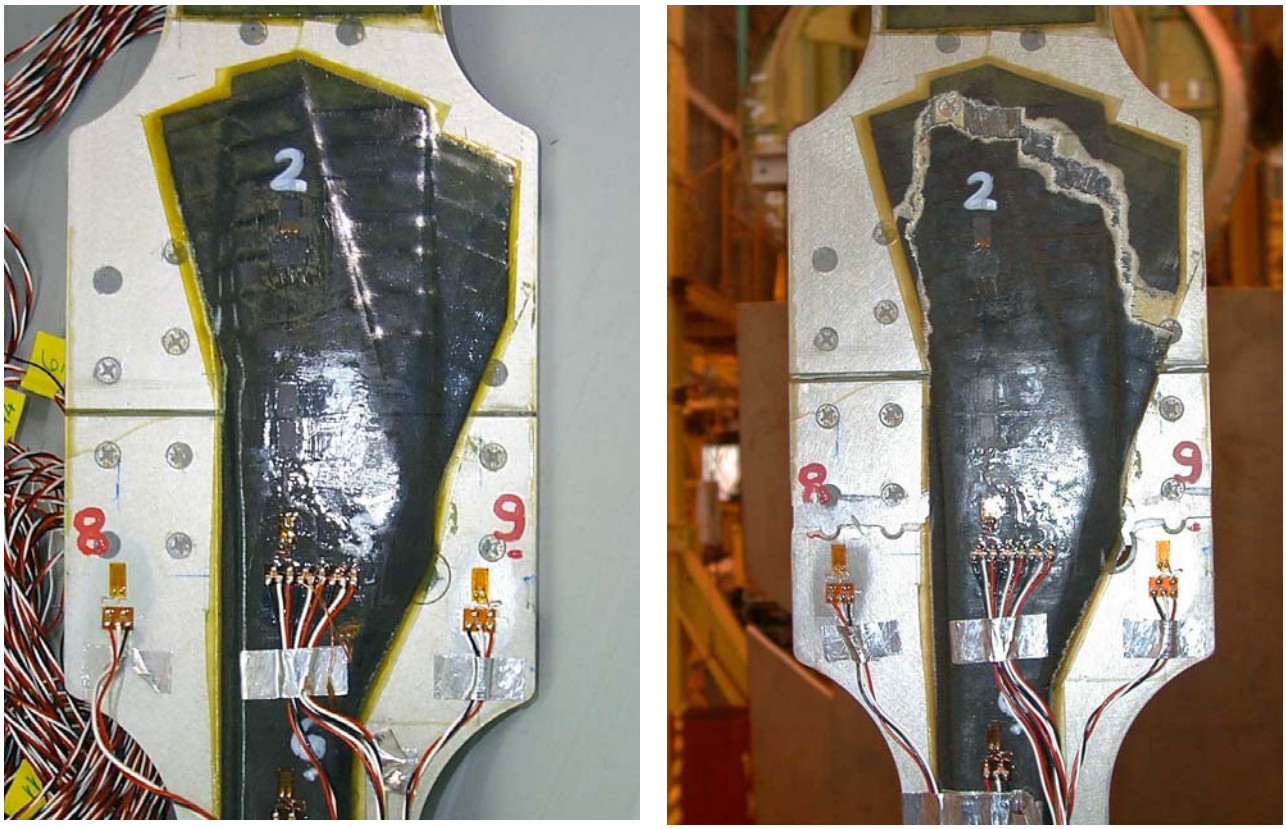

Figure 10: Static test specimen before and after failure

A test specimen, representing the repair and original structure at STA 341, was designed. A total of 4 static and fatigue tests were performed. One specimen was statically tested up to failure and all others were tested in fatigue. No indications of damage were found in the patch after ultimate loads were applied. The static test specimen failed slightly above 150% Limit load. The failure mode can be seen in Figure 10. The fatigue test with initial crack at a fastener hole demonstrated very low crack growth rate (1mm for 1000 flight hours).

A qualitative strain survey at the repair area was performed on the aircraft. Strain readings were taken before and after applying the repair on the aircraft. Good correlation between the analytical prediction and test results was observed.

Based on the analytical and experimental substantiation described above, it was concluded that the repair has sufficient life to be implemented as a temporary repair of cracked skin on the F-16 aircraft. The repair has flown more than 100 flight hours on an F-16 in service with the IAF.

IAF and IAI demonstrated the ability of repairing a critical metal F-16 structure with a bonded Boron epoxy co-cured patch. The repair can be implemented on a cracked skin as a temporary repair, ensuring the required static strength and life extension. It can also be implemented as a preventative repair. The repair concept was successfully tested both on the aircraft and by means of component tests.

The results of this study were presented at the 43rd Israel Annual Conference on Aerospace Sciences [11] and will be presented in a paper to be given at the 22nd ICAF Symposium [12].

11.4 COMPOSITE MATERIALS

11.4.1 COMPRES: EU Funded Multi-National Research Effort for Bonded Composite Repairs of Aging Commercial Aircraft (A. Nathan, H. Leibovich, I. Kressel, IAI)

Bonded composite repairs have been proven as excellent candidates to be used both as preventative measures to ensure that damage will not initiate at critical locations, as well as a proven method for retarding future growth of existing damage.

A multi-national multi-year research effort was initiated in 1999 for this subject under the auspices of the European Commission BRITE-EURAM combined research projects. The research effort included nine industries, research institutes and universities in six different countries. HAI of Greece was in charge of overall management of this Brite-Euram 4th framework project, IAI served as the technical coordinator. The consortium included aircraft manufacturers, maintenance facilities, composite material suppliers, repair equipment manufactures, universities and research institutes from France, England, Italy, Portugal, Israel and Greece.

At the 20th ICAF Symposium (1999), the objectives, scope and tasks were presented for the COMPRES project. The program was then just at the beginning stages, thus mainly considerations and direction of planned project progress were presented. As the program now has been completed, we are able to present a more in-depth technical report regarding:

- *stress intensity factor calculations for cracks under composite patches*
- *patch design criteria*
- *NDE round robin results (thermography, shearography, ultrasonics, ...)*
- *surface preparation*
- *validation test results*
- *development of repair equipment*
- *innovative curing process*
- *commercial aging aircraft damage assessment*
- *preparation of a repair technical manual*

The subject of bonded composite repairs is not new. Composite structural repairs and reinforcement of military aircraft structure have been applied for well over 20 years. There has also been a significant effort in the past years in both Australia and the U.S. to expand the application to the commercial aircraft arena. Nevertheless, the *COMPRES* project has made some important innovative headway regarding the following subjects:

- *3D "p-version" parametric finite element analysis to calculate stress intensity of the crack under the composite patch*
- *treatment of residual stresses induced by the thermal mismatch problem between the composite material patch and the aluminum parent material*
- *innovative curing equipment*
- *improved surface treatment equipment*
- *repair manual for characteristic damaged structure*
- *statistical data reduction of damage prone primary structure*

The results of this study will be presented in a paper to be given at the 22nd ICAF Symposium [13]. The purpose of the paper is to present the results, technical progress and lessons learned during the *COMPRES* project and to emphasize the innovative aspects that have the most relevance to the fatigue community. Figure 11 shows a typical bonded composite repair that was experimentally evaluated. Figure 12 contains measured crack growth behavior of a repaired aluminum structure compared to analytical predictions.

Figure 11: Typical Bonded Composite Repair that was Experimentally Evaluated

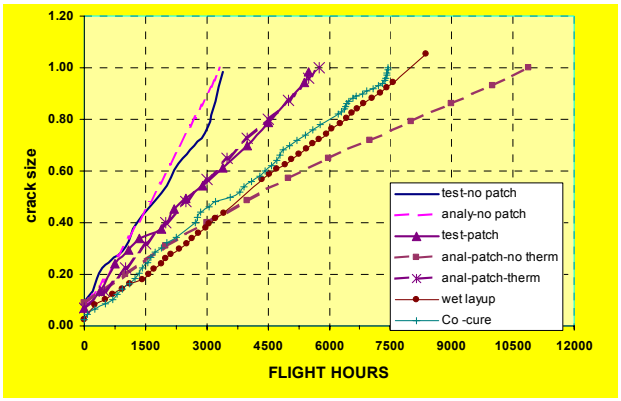

Figure 12: Measured Crack Growth Behavior of a Repaired Aluminum Structure Compared to Analytical Predictions

11.4.2 Fatigue of Composite Materials (Z. Granot, IAI and S. Gali, Consultant)

An extensive literature review was carried out concerning the fatigue of composite materials. The previously widely accepted damage tolerance design criteria of limiting the strain under ultimate loading to roughly 3000 με, gradually increased to higher values over the years, as improved materials emerged. However, it appears that in recent years this type of design criteria is no longer considered sufficiently reliable or consistent with minimum weight design. Instead there is today a shift in favor of applying one of the following two approaches in the substantiation of the composite structure for fatigue.

The first approach is a safe-life fatigue, or a "No Growth" assessment, where the original residual strength of the structure is not allowed to degrade, in the presence of barely visible impact damage flaws, to below ultimate capability.

The second approach is a damage-tolerance type approach, or a damage growth type assessment, which aims at eventually establishing inspection intervals, and which ensures that the residual strength of the structure is equal or greater than limit loads. This method is more popular for substantiation by testing, but difficult to implement analytically.

In general, fatigue analysis methods can be divided into several methods, methods that monitor the change in material modulus, methods for monitoring degradation of residual strength, methods for monitoring flaw growth (fracture mechanics), and empirical methods for predicting fatigue life using S-N curves and constant-life diagrams.

The main thrust of the proposed continuing work at IAI is to establish an analytical "No Growth" capability based on established principles and in-house fatigue test data that are to be established by a fatigue test program that is to be carried out shortly.

11.4.3 Evaluation of Heat Damage in Graphite-Epoxy Solid Laminates and Honeycomb Structures (S. Girshovich, U. Sol and V. Weisberg, IAI)

During operational service, advanced composite aircraft assemblies can be exposed to high temperature, which may cause degradation of mechanical properties.

Heat damage may occur as a result of:

1. Failure in one of the hot air tubes (for instance anti-ice system)
2. Fire in the engine area
3. During field repairs (failure of heating blanket)
4. Lightning strikes
5. Fire in the vicinity of the aircraft. (particularly during battle)

Israel Aircraft Industries (IAI) and Israel Air Force (IAF) did not have the appropriate tools to measure the effect of overheating on the degradation of mechanical properties.

The purpose of this study was to evaluate the damage caused to graphite-epoxy laminate and sandwich structures due to deferent levels of heat exposure and to correlate the physical and mechanical properties degradation with non-destructive evaluation results.

The experiments where made on the following materials and structures:

- Gr/Ep Laminates, 125°C (Vicotex 913) - 3,5,7,10 plies (0.72 – 2.4 mm)
- Gr/Ep Laminates, 175ºC (Hexcel 3502) – 10 plies (1.9 mm)
- Sandwich panels made of 3 plies of Vicotex 913 (thickness 0.72 mm) bonded to HRH 3.0, 3/16 thick Nomex honeycomb (co-cured).

During the experiments, the influence of the maximum temperature, temperature rate and heating time on the composite materials damage was evaluated.

The study evaluated heat damage in graphite-epoxy solid laminates (125ºC) at temperature ranges of:

- 25ºC-180ºC - Low temperature
- 180ºC-230ºC – Moderate temperature
- 230º C and up – High temperature

For honeycomb structure, the temperature range was 180ºC - 340ºC

The heated panels were evaluated using the following NDE methods:

- **Visual**
- **NDE**
  - Pulse Echo A-Scan assisted with signal analysis
  - Through Transmission C-Scan assisted with image analysis
  - Infrared
  - SMS - Sensitive Motion Sensor

  (Note: SMS is based on a new ultrasonic sensor, which is being evaluated.)
- **Mechanical**
  - Inter Laminar Shear Stress
  - Compression
  - Special Short Four Point Bending test specimen
  - Special Torsion Short beam test specimen.
- **Hot Wet**
  - Compression using IITRI

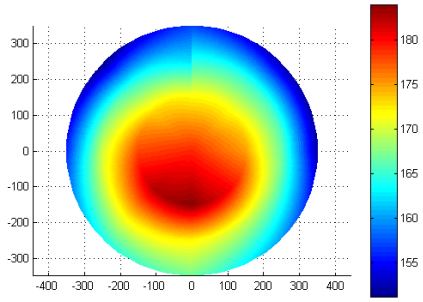

Figure 13: Temperature Distribution Measurements

- **Physical**
  - Tg
  - TGA
  - Resin Contents
- **Microscope**
  - Optical microscope
  - SEM

Figure 13 shows the temperature distribution of an overheated sandwich panel, as measured by several thermocouples.

The results of this study are currently being evaluated and final conclusions will be published at a later date.

11.4.4 Tension-Compression Electromechanical Fatigue Behavior of Graphite/Epoxy Laminate with Embedded Piezoelectric Actuator (M. Yocum and H. Abramovich, Technion)

Very little research has been done in the field of structural integrity of smart structures, yet it is a key component of study if one is to fully understand the structural implications of load bearing structures used in conjunction with smart materials. One important field in structural integrity studies is fatigue of piezoelectric (PZT) actuated structures. To date, virtually all research related to fatigue of smart structures has either focused on mechanical fatigue of the structure with an inactive PZT (or some other material simulating an inactive piezoelectric), or mechanical fatigue studies on the PZT itself, cycling loads directly on a piezoelectric and then checking its ability to serve as sensor or actuator. Almost no work has been done in the combined mechanical fatigue of the structure while actuating the PZT, a phenomenon called electromechanical (E/M) fatigue.

This study seeks to determine the functionality and life of a piezoceramic actuator/sensor embedded in composite while undergoing a combined electromechanical fatigue under fully reversed, tension-compression fatigue conditions. The E/M fatigue behavior of a quasi-isotropic graphite/epoxy laminate with embedded piezoelectric QP15N transducer (made by Cymer Inc) was investigated. PZT was inserted in the cutout area of the middle two plies of a $[0/\pm45/90]_S$ lay-up. Every fatigue test was conducted with a triangular loading waveform at a frequency of 10 Hz and the fully reversed stress ratio of R = –1. Different stress levels were tested ranging from one-half to twice the design limit suggested by the manufacturer of the PZT; the design limit for this PZT is 1000 με (nominally 50 MPa), therefore fatigue tests were run load-control at individual stresses ranging from 25 MPa (500 με) to 100 MPa (2000 με). At the same time, the embedded PZT was subjected to AC voltage ranging from –100 V to 100 V or 100 V to -100 V at 10 Hz, giving either an in-phase or out-of-phase electrically induced strain with respect to the mechanical loading or strain.

Periodically, the output voltage of the piezoelectric was checked during cycling to determine the health of the PZT as a sensor. Failure of the PZT was assumed when a reduction of 30% of the original output voltage was seen after repoling the piezoelectric.

A final set of tests was run with only mechanically induced strain on the structure, again checking the health of the PZT throughout each test. These results were compared with the E/M fatigue test results to determine the additional extent of damage E/M fatigue adds to the functionality of a piezoelectric sensor.

Finally, the results were compared with results from a series of tension-tension E/M fatigue results. In these tests, the material system and type of piezoelectric were the same. Only the electrical and mechanical loading profiles were different to remain in tension the entire test.

The results of this study were presented at the 43rd Israel Annual Conference on Aerospace Sciences [14].

11.5 MISCELLANEOUS

11.5.1 Finite-Element Analysis of a Riveted Joint (D. Barlam, IAI)

Riveted splice joints are very complex structure to analyze. Rigorous procedures need to be developed in order to assess and verify their fatigue life. There exist some simplified numerical procedures, based upon analytical or numerical approach. Usually they ignore the fact that the problem, in essence, is three-dimensional and, moreover is non-linear. The later stems from the fact that the rivet-hole interaction is a problem of contact where neither contact forces nor displacements and areas of contact are known beforehand.

In the present work full 3D Finite Element Analysis of a rivet joint connection was conducted by means of widely used commercial code MSC.NASTRAN. To model the rivet-hole interaction, slide line type of boundary conditions were used. This type of boundary condition allows simulating contact between deformable bodies.

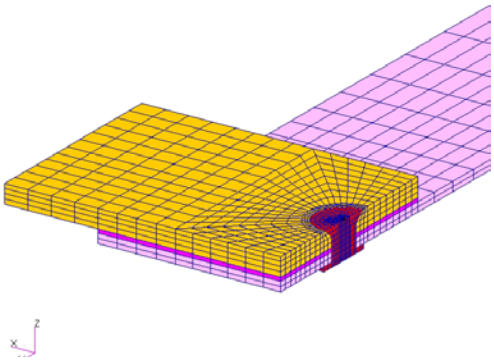

Both the rivet and details were modeled by CHEXA 3D elements. The other boundary conditions (loads and constraints), applied to the local model, were obtained from the global model.

3D models (including contact between rivet and attached plates) provide more realistic stress distribution around the hole. Figure 14 shows the finite-element model that was used for this study. Figure 15 describes the three-dimensional stress distribution around the hole, displacements and contact under loading. The data obtained from this study were used for the life expectancy prediction of riveted connections.

Figure 14: FEM Used in the Study

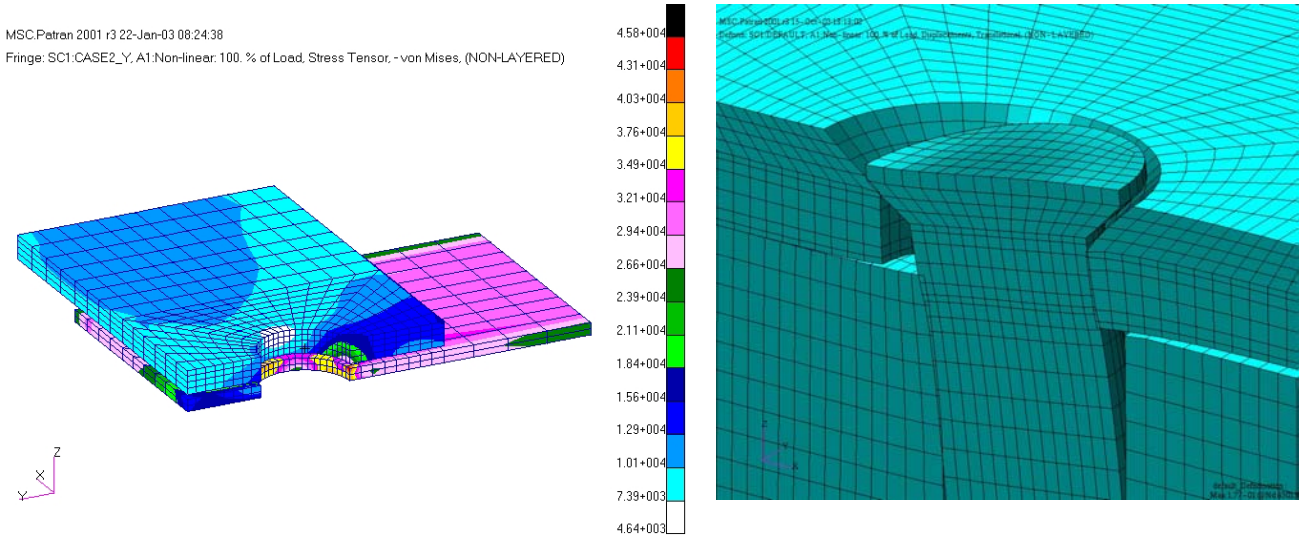

Figure 15: Three-Dimensional Stress Distribution, Displacements and Contact of Elements

11.5.2 Study and Evaluation of N.D.E. Methods for Corrosion Detection (S. Girshovich and U. Sol, IAI)

The previous Israel National Review [1] described a study dealing with the detection of corrosion using various NDE methods. The present study continued this investigation and extended the study to include new methods that are presently in the stage of development. In order to determine the effectiveness of the NDE methods, special samples were design and manufactured. The samples represent different severity levels of pitting and exfoliation corrosion.

These samples were tested using the following methods: Radiographic X-ray, Eddy-Current, ComScan, Magneto-Optic, MWM (Meandering Winding Magnetometer), Radiographic neutron and Ultrasonic Resonance. An assessment of these methods and a comparison of their ability to detect, estimate the severity of the corrosion, inspect large areas and the relative cost advantage of each method was evaluated. Some of the evaluations were made using IAI's equipment and in the other cases (especially the novel applications) the reference standards were sent to the developer and his results were incorporated.

The following parameters were evaluated for each method:

- Detection of corrosion without component **Disassembly**.
- **Accessibility** of the instruments to the inspection area
- **Sensitivity** to detect different severity grades
- Estimation of corrosion penetration **Depth**
- The **Cost** of the inspection
- The ability to distinguish between corrosion and **Artifacts**
- **Safety** of inspection

Results of Methods Evaluation:

Method / Abilities	Radio. X-Ray	Eddy Current	Magneto Optic	Com Scan	Radio. Neutron	Thermal	Resonance	MWM
Disassembly	1	2	2	3	1	2	2	2
Accessibility	1	4	4	1	5	4	4	4
Sensitivity	2	3	4	4	5	--	--	--
Depth	2	3	1	1	5	4	4	2
Cost	2	1	2	5	4	--	--	--
Artifacts	2	2	4	5	4	--	--	--
Safety	2	5	5	2	1	5	5	5

Note: Comparisons should only be between the same categories, see below.

Disassembly	5 -	Not Required	1 -	Full required
Accessibility	5 -	Easy	1 -	Complicated
Sensitivity	5 -	High sensitivity	1 -	Low Sensitivity
Depth	5 -	High capability	1 -	Low capability
Cost	5 -	Inexpensive	1 -	Expensive
Artifacts	5 -	High capability	1 -	Low capability
Safety	5 -	Safe	1 -	Special precautions

The methods were divided in to three categories:

1. Widespread methods – Radiographic X-Ray, Eddy current, Magneto optic
2. Limited use – ComScan, Radiographic Neutron
3. Novel Applications – Thermal, Ultrasonic Resonance, MWM

11.5.3 Computation of Stress-Intensity Functions in the Neighborhood of Edges (Z. Yosibash et al, Ben-Gurion University)

The computation of stress-intensity functions in the neighborhood of edges in a three-dimensional linear elastic body is of major importance in engineering practice, and some methods for extracting these from finite-element solutions have been earlier proposed. However, a detailed mathematical framework of the 3-D edge singularities seems not to be available, and the methods are not the most efficient and accurate due to the need of extracting the Edge Flux Intensity Functions (EFIFs) very close to the edges.

Towards developing efficient and accurate methods, we consider in [15] the solution of the Laplace equation on 3-D domains in the vicinity of straight edges. This is because both Laplace and elasticity problems are elliptic and therefore their solutions have similar characteristics. The solution to the Laplace operator in three-dimensional domains in the vicinity of straight edges is presented as an asymptotic expansion involving eigen-pairs with their coefficients called EFIFs. The eigen-pairs are identical to their two-dimensional counterparts over a plane perpendicular to the edge.

Extraction of EFIFs however, cannot be obtained in a straightforward manner over this two-dimensional plane. A method based on L^2 projection and Richardson extrapolation is presented for point-wise extraction of EFIFs from p-finite element solutions and illustrated by examples.

A similar but more efficient method, based on ``energy projection'', for extracting EFIFs is proposed. In [16] a general framework of very efficient extraction of Edge Flux/Stress Intensity Functions along edges is proven mathematically based on generalization of the dual-singular extraction method in 2-D domains (or the so called Contour Integral Method).

11.5.4 Solutions of Linear Elastostatic Problems in the Vicinity of Reentrant Corners or Multi-Material Interfaces (Z. Yosibash et al, Ben-Gurion University)

A research project reported in [17] and [18] is directed to solutions of linear elastostatic problems in the vicinity of reentrant corners, or multi-material interfaces, and the formulation of a failure criterion for these problems. The validity of three ``best'' failure criteria proposed in the last decade for prediction of failure initiation at V-notch sharp tips has been examined and compared with experimental observations, and a new and simplified one is proposed in [17]. The experiments include: loading of specimens made of two kinds of elastic materials (PMMA - a polymer, and Al_2O_3-7%ZrO_2, a composite ceramic) in three and four-points, so to produce mode I stress field in the vicinity of the notch tip. To quantify the influence of V-notch tip radius on the failure initiation, specimens having different tip radii have been selected.

All failure criteria assume a mathematical sharp tip, however a small blunt tip shows a higher generalized stress intensity factor as compared to the predicted values.

Nevertheless, both the Novoshilov-Seweryn and Leguillon criteria seem to predict well the observed failures, however, as the opening angle increases, their validity deteriorates. Leguillon criterion outperforms the Novoshilov-Seweryn criterion, and it has been refined so to match better the experimental observations [18].

A sample of the many p-version finite-element models simulating the Al_2O_3-7%ZrO_2 tested specimens together with the extracted eigen-pairs and generalized stress intensity factors [17] is shown in Figure 16, and the prediction (by Novozhilov-Seweryn and Leguillon's criteria) vs. the experimental generalized stress-intensity factor, as a function of the V-notch opening angle [17] is shown in Figure 17.

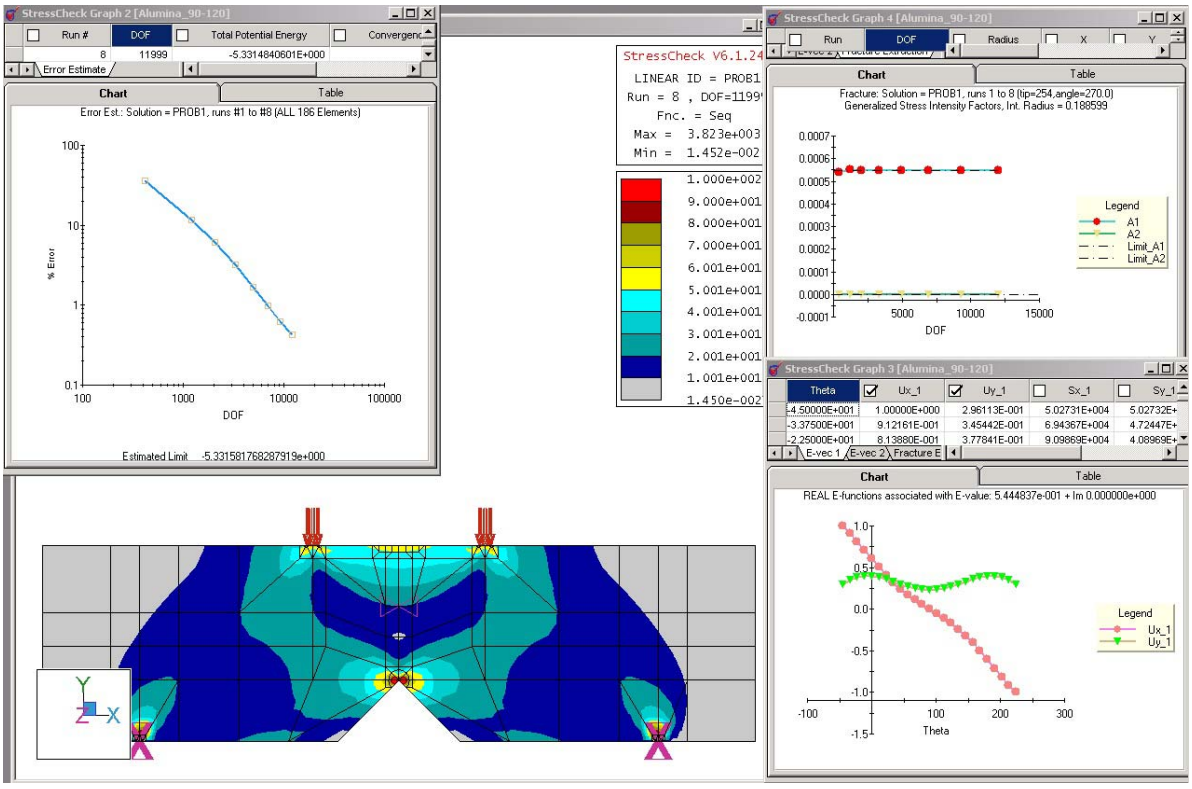

Figure 16: Typical Finite-Element Model of a Composite Ceramic Specimen

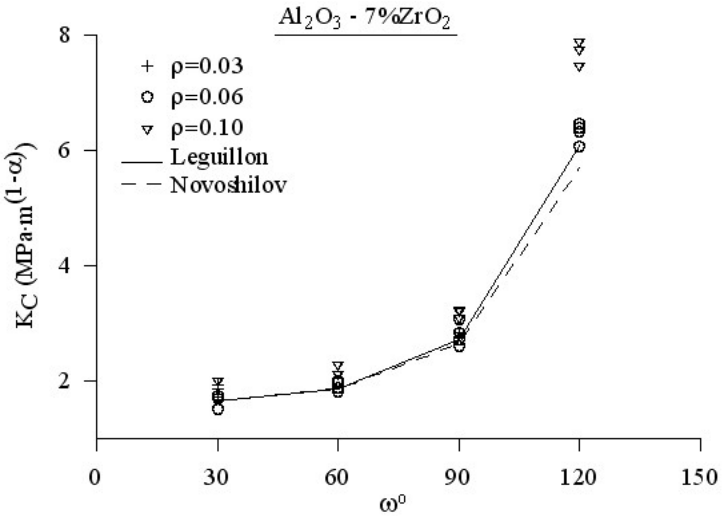

Figure 17: Predicted vs. Experimentally Measured V-notch Opening Angle

11.5.5 Fracture Mechanics of Bonded Joints (L. Banks-Sills et al, Tel-Aviv University)

The reliability of a joint subjected to mechanical and thermal loads during processing and service constitutes a major technical problem. Joints contain flaws and the observed strength of a joint depends upon the location and size of the flaws, as well as the crack path through the joint. The behavior of a crack within an epoxy layer joining two aluminum adherends is described in [19-21].

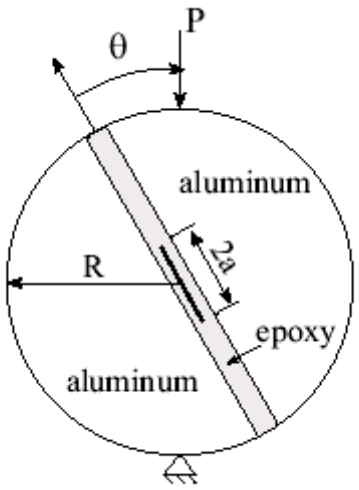

The purpose of these investigations was to measure the fracture toughness of a crack within an adhesive joint and consider its crack path. Sandwich Brazilian disk specimens (Figure 18) made of two aluminum substrates joined by a thin layer of epoxy were employed in the testing. A paraffin notch was located within the adhesive layer. The advantage of this specimen type is that it provides a wide range of mode mixity.

Stress-intensity factors at fracture were obtained from a finite-element analysis of each specimen to account for layer thickness, position of the crack within the layer relative to the adherends, crack length and loading angle. It was found that stress-intensity factors obtained from an asymptotic analysis did not describe well the geometry employed here due to the relative dimensions of the specimen (mainly layer thickness). The residual stresses were calculated and seen to be parallel to the crack. Thus, the stress-intensity factors were not affected by this stress.

Figure 18: Brazilian Disk Sandwich Specimen

It may be noted that the notch was placed nearly in the middle of the bond. For most loading angles, the crack propagated into the lower interface. For two loading angles in which $K_{II}=K_I < 0{:}9$ at failure, the crack began to propagate within the glue, but then ran into the lower interface. This short propagation did not appear to change the critical energy release rate at failure for these specimens.

The "T-stress criterion" for cracks in bonded joints does not appear appropriate for the Brazilian disk specimen since K_{II} is nearly constant with respect to position of the crack within the bond. The maximum tangential stress criterion of Erdogan and Sih predicted well the general direction of crack propagation. Further experiments are required to measure the exact direction of crack propagation in order to compare to this theory. It should be noted that the crack path influences the fracture toughness. Hence, it is important that the crack path of the problem to be analyzed and specimen employed for testing be the same.

The epoxy was seen to be brittle from both the stress-strain tests, as well as the fracture toughness tests of the bulk epoxy where G_{IC}, the critical energy release rate in mode I or the fracture toughness, was found to be 53.0 N/m. For the sandwich specimens a G_{IC} value of 19.9 N/m was obtained. This value is approximately 40% that of the bulk epoxy. Measurements showed the critical energy release rate of the bulk epoxy to be somewhat higher than that for the in-layer path in the sandwich structure. Other investigators found G_{IC} of the bulk epoxy to be lower than that in the sandwich specimen even when the crack propagated within the epoxy. Perhaps the low critical energy release rate values obtained from the sandwich specimens for small values of the loading angle θ are a result of the crack propagating into the interface; this would be similar to the phenomenon observed in the literature.

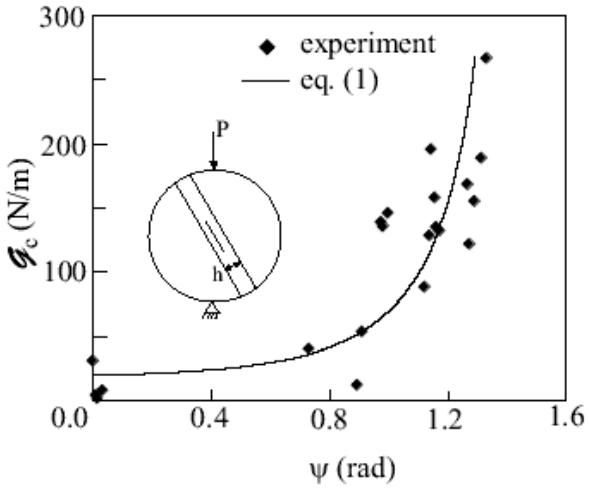

Figure 19: Critical Energy Release Rate as a Function of Phase Angle

The G_C values of the sandwich structure were seen to increase with increasing mode mixity, as may be observed in Figure 19. This was also seen for interface cracks in other investigations.

In Figure 19, there is scatter about the curve, which was explained in part by the differences in layer thickness between the specimens. The influence of layer thickness was also observed in other investigations for interface cracks in a sandwich structure. There may be additional explanations for the scatter, including in particular different epoxy batches, adherend surface preparation, differences in temperature and humidity during testing.

11.6 REFERENCES

1. Brot, A., "Review of Aeronautical Fatigue Investigations in Israel, April 1999 – March 2001", *Minutes of the 27th ICAF Conference,* Toulouse, France, 2001.

2. Altus, E., and Konstantino, E., "Optimum Laser Surface Treatment of Fatigue Damaged Ti-6Al-4V Alloy", *Materials Science and Engineering,* A302, 2001.

3. Altus E., 2002, "Nonlinear differential equation for fatigue damage evolution by a micromechanic model ", Mechanics Of Materials, 34(5): 257-266

4. Altus E., Gerstman Z., Golubchick A., 2002, "Two Level Fatigue Loading (H-L) of Mg Alloys: Micromechanic Modeling vs. Experiments", Metallurgical Science and Technology, 20(2): 3-8

5. Perl, M. and Nachum, A., "3-D Stress Intensity Factors for Internal Cracks in an Overstrained Cylindrical Pressure Vessel – Part I: The Effect of Autofrettage Level", *Journal of Pressure Vessel Technology,* ASME, Vol. 122, November 2000.

6. Perl, M. and Nachum, A., "3-D Stress Intensity Factors for Internal Cracks in an Overstrained Cylindrical Pressure Vessel – Part II The Combined Effect of Pressure and Autofrettage", *Journal of Pressure Vessel Technology,* ASME, Vol. 123, February 2001.

7. Perl, M., Levy, C., and Ma, Q., "The Influence of Multiple Axial Erosions on the Fatigue Life of Autofrettaged Pressurized Cylinders", *Journal of Pressure Vessel Technology,* ASME, Vol. 123, August 2001.

8. Perl, M., Levy, C., and Ma, Q., "The Influence of Multiple Axial Erosions on a Three-Dimensional Crack in Determining the Fatigue Life of Autofrettaged Pressurized Cylinders", *Journal of Pressure Vessel Technology,* ASME, Vol. 124, February 2002.

9. Brot, A and Matias, C., "An Evaluation of Several Retardation Models for Crack Growth Prediction under Spectrum Loading", *Proceedings of the 2002 USAF Aircraft Structural Integrity Program* Conference, 2002.

10. Brot, A. and Matias, C., "Crack Growth Predictions Using Several Retardation Models", *Proceedings of the 43rd Israel Annual Conference on Aerospace Sciences,* 2003.

11. Kressel, I., Cohen, I. et al, "Design Substantiation and Application of a Boron-Epoxy Patch Repair on an F-16 Upper Fuselage Skin", *Proceedings of the 43rd Israel Annual Conference on Aerospace Sciences,* 2003.

12. Kressel, I., Cohen, I. et al, "Design Substantiation and Application of a Boron-Epoxy Patch Repair on an F-16 Upper Fuselage Skin", *Proceedings of the 22nd ICAF Symposium,* 2003.

13. Nathan, A., Leibovich, H. and Kressel, I., "COMPRES: EU Funded Multi-National Research Effort for Bonded Composite Repairs of Aging Commercial Aircraft", *Proceedings of the 22nd ICAF Symposium,* 2003.

14. Yokum, M., Abramovich, H., et al, "Electromechanical Fatigue Behavior of Graphite/Epoxy Laminate with Embedded Piezoelectric Actuator", *Proceedings of the 43rd Israel Annual Conference on Aerospace Sciences,* 2003.

15. Yosibash, Z., Actis, R. and Szabo, B.A.,``Extracting Edge Flux Intensity Functions for the Laplacian", International Journal for Numer. Meth. Engrg., 53, No. 1, 2002.

16. Costabel, M., Dauge, M. and Yosibash, Z.,``A quasidual function method for the computation of stress intensity factors along edges", Submitted for publication, 2002.

17. Yosibash, Z., Bussiba, A. and Gilad, I., ``Failure Criteria for Brittle Elastic Materials", Submitted for publication, 2002.

18. Leguillon, D. and Yosibash, Z., ``Crack onset at a V-notch. Influence of the notch tip radius.", Submitted for publication, 2002.

19. Banks-Sills, L. and Schwartz, J., "Crack Paths in Adhesive Bonds", in: *Recent Advances in Experimental Mechanics - In Honor of Professor I.M. Daniel*, ed. E.E. Gdoutos, Kluwer Academic Publishers, Netherlands, 2002.

20. Banks-Sills, L., Schwartz, J. and Fourman, V., "Measurement of Fracture Properties of Bonded Joints", in*: Structural Integrity and Fracture*, eds. A.V. Dyskin, X. Hu, E. Sahouryeh, A.A. Balkema Publishers, Tokyo, 2002.

21. Banks-Sills, L. and Schwartz J., "Fracture Testing of Brazilian Disk Sandwich Specimens", to appear: *International Journal of Fracture*.